Inorg. Chem. **2005**, *44*, 9547–9553

Neutral and Ionic Complexes of C_{60} with Metal Dibenzyldithiocarbamates. Reversible Dimerization of $C_{60}^{\bullet-}$ in Ionic Multicomponent Complex $[Cr^{I}(C_6H_6)_2^{\bullet+}]\cdot(C_{60}^{\bullet-})\cdot 0.5[Pd(dbdtc)_2]$

Dmitri V. Konarev,*[,†,‡] Andrey Yu. Kovalevsky,[§] Akihiro Otsuka,[†,£] Gunzi Saito,*[,†] and Rimma N. Lyubovskaya[‡]

Division of Chemistry, Graduate School of Science, Kyoto University, Sakyo-ku, Kyoto 606-8502, Japan, Institute of Problems of Chemical Physics RAS, Chernogolovka, Moscow region 142432, Russia, Department of Chemistry, State University of New York at Buffalo, Buffalo, New York 14260, Research Center for Low Temperature and Materials Sciences, Kyoto University, Sakyo-ku, Kyoto 606-8502, Japan

Received July 27, 2005

New molecular complexes of C_{60} with metal(II) dibenzyldithiocarbamates, $M(dbdtc)_2\cdot C_{60}\cdot 0.5(C_6H_5Cl)$, where M = Cu^{II}, Ni^{II}, Pd^{II}, and Pt^{II} (**1**–**4**) and an ionic multicomponent complex $[Cr^{I}(C_6H_6)_2^{\bullet+}]\cdot(C_{60}^{\bullet-})\cdot 0.5[Pd(dbdtc)_2]$ (**5**) (Cr-$(C_6H_6)_2$: bis(benzene)chromium) were obtained. According to IR, UV–visible–NIR, and EPR spectra, **1**–**4** involve neutral components, whereas **5** comprises neutral $Pd(dbdtc)_2$ and $C_{60}^{\bullet-}$ and $Cr^{I}(C_6H_6)_2^{\bullet+}$ radical ions. The crystal structure of **5** at 90 K reveals strongly puckered fullerene layers alternating with those composed of $Pd(dbdtc)_2$. The $Cr^{I}(C_6H_6)_2^{\bullet+}$ radical cations are arranged between the layers. Fullerene radical anions form pairs within the layer with an interfullerene C···C contact of 3.092(2) Å, indicating their monomeric state at 90 K. This contact is essentially shorter than the sum of van der Waals radii of two carbon atoms, and consequently, $C_{60}^{\bullet-}$ can dimerize. According to SQUID and EPR, single-bonded diamagnetic $(C_{60}^{-})_2$ dimers form in **5** below 150–130 K on slow cooling and dissociate above 150–170 K on heating. The hysteresis was estimated to be 20 K. For the $(C_{60}^{-})_2$ dimers in **5**, the dissociation temperature is the lowest among those for ionic complexes of C_{60} (160–250 K). Fast cooling of the crystals within 10 min from room temperature down to 100 K shifts dimerization temperatures to lower than 60 K. This shift is responsible for the retention of a monomeric phase of **5** at 90 K in the X-ray diffraction experiment.

Introduction

Fullerenes form a wide variety of molecular and ionic donor−acceptor complexes with organic and organometallic donors[1] such as aromatic hydrocarbons,[2] substituted tetrathiafulvalenes,[3] amines,[3c,4] metallocenes,[1,5] porphyrins and metalloporphyrins,[6] porphyrazines,[7] and other compounds.[1,3c] Both ferromagnetism[4a] and a reversible formation of σ-bonded structures[5e−g] are observed in ionic compounds. Neutral complexes are promising photoactive compounds since they form excited ionic states[8a] and manifest photoconductivity[8b]

* To whom correspondence should be addressed. E-mail: konarev@icp.ac.ru (D.V.K); saito@kuchem.kyoto-u.ac.jp (G.S.).

† Division of Chemistry, Graduate School of Science, Kyoto University, Japan. Fax: +81-75-753-40-35.

‡ Institute of Problems of Chemical Physics RAS, Chernogolovka, Moscow region 142432, Fax: +007-096-515-54-20.

§ Department of Chemistry, State University of New York at Buffalo.

£ Research Center for Low Temperature and Materials Sciences, Kyoto University.

(1) (a) Balch, A. L.; Olmstead, M. M. *Chem. Rev.* **1998**, *98*, 2123. (b) Konarev, D. V.; Lyubovskaya, R. N. *Russ. Chem. Rev.* **1999**, *68*, 19. (c) Reed, C. A.; Bolskar, R. D. *Chem. Rev.* **2000**, *100*, 1075.

(2) (a) Pénicaud, A.; Carreón, O. Y.; Perrier, A.; Watkin, D. J.; Coulon, C. *J. Mater. Chem.* **2002**, *12*, 913. (b) Litvinov, A. L.; Konarev, D. V.; Kovalevsky, A. Yu.; Neretin, I. S.; Slovokhotov, Yu. L.; Coppens, P.; Lyubovskaya, R. N. *CrystEngCommun.* **2002**, *4*, 618.

(3) (a) Izuoka, A.; Tachikawa, T.; Sugawara, T.; Suzuki, Y.; Konno, M.; Saito, Y.; Shinohara, H. *J. Chem. Soc., Chem. Commun.* **1992**, 1472. (b) Saito, G.; Teramoto, T.; Otsuka, A.; Sugita, Y.; Ban, T.; Kusunoki, M.; Sakaguchi, K. *Synth. Met.* **1994**, *64*, 359. (c) Konarev, D. V.; Lyubovskaya, R. N.; Drichko, N. V.; Yudanova, E. I.; Shulga, Yu. M.; Litvinov, A. L.; Semkin V. N.; Tarasov, B. P. *J. Mater. Chem.* **2000**, 803.

(4) (a) Allemand, P.-M.; Khemani, K. C.; Koch, A.; Wudl, F.; Holczer, K.; Donovan, S.; Grüner, G.; Thompson, J. D. *Science* **1991**, *253*, 301. (b) Konarev, D. V.; Kovalevsky, A. Yu.; Litvinov, A. L.; Drichko, N. V.; Tarasov, B. P.; Coppens, P.; Lyubovskaya, R. N. *J. Solid State Chem.* **2002**, *168*, 474. (c) Nadtochenko, V. A.; Moravskii, A. A.; Gritsenko, V. V.; Shilov, G. V.; D'yachenko, O. A. *Mol. Cryst. Liq. Cryst. Sci, Technol., Sec. C* **1996**, *7*, 103.

10.1021/ic051261i CCC: $30.25
Published on Web 11/05/2005

under photoexcitation. Recently, we have shown a butterfly-shaped copper(II) diethyldithiocarbamate dimer, $[Cu^{II}(dedtc)_2]_2$, to cocrystallize with C_{60} to produce $[Cu^{II}(dedtc)_2]_2 \cdot C_{60}$ with a closely packed layered structure. The excitation of the crystal of $[Cu^{II}(dedtc)_2]_2 \cdot C_{60}$ by white light enhances photocurrent by a factor of 100.[9] To extend this work, we studied the cocrystallization of C_{60} with bulky metal(II) dibenzyldithiocarbamates, $M(dbdtc)_2$. Moreover, ionic $(D_1^{\bullet+}) \cdot (\text{fullerene}^{\bullet-}) \cdot (D_2)$ complex was obtained using a multicomponent approach: D_1 is a strong donor of small size potentially able to ionize fullerene in solid state, and D_2 is a large neutral $M(dbdtc)_2$ molecule defining a supramolecular packing pattern. Bis(benzene)chromium ($Cr(C_6H_6)_2$), tetrakis(dimethylamino)ethylene (TDAE), decamethylchromocene (Cp^*_2Cr), and decamethylcobaltocene (Cp^*_2Co) were used as D_1 components and cobalt(II) tetraphenylporphyrinate ($Co^{II}TPP$), cyclotriveratrylene (CTV), and *N*,*N*′,*N*′,*N*′-tetrabenzyl-*p*-phenylenediamine (TBPDA) were used as D_2 components.[10] We found unusual diamagnetic σ-bonded ($Co^{II}TPP \cdot \text{fullerene}^-$) anions in $(D^+) \cdot (Co^{II}TPP \cdot C_{60}^-) \cdot$solvent (D is $Cr(C_6H_6)_2$[10a] and TDAE[10b]), and single-bonded $(C_{60}^-)_2$ and $(C_{70}^-)_2$ dimers in $(Cs^+)_2 \cdot (C_{60(70)}^-)_2 \cdot CTV \cdot (DMF)_x$ (DMF: *N*,*N*′-dimethylformamide; $x = 5-7$).[10c-d] TBPDA forms $(D^+) \cdot (C_{60}^{\bullet-}) \cdot 2(\text{TBPDA})$ complexes (D: Cp^*_2Cr, Cp^*_2Co, and TDAE), which exhibit a short-range antiferromagnetic interaction of spins.[10b,e]

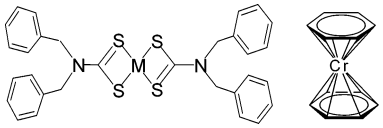

Figure 1. Molecular components used for the preparation of **1**−**5** (M = Cu^{II}, Ni^{II}, Pd^{II}, and Pt^{II}).

In this work, we present neutral complexes of C_{60} with metal(II) dibenzyldithiocarbamates, $M(dbdtc)_2 \cdot C_{60} \cdot 0.5(C_6H_5Cl)$, where M = Cu^{II}, Ni^{II}, Pd^{II}, and Pt^{II} (**1**−**4**) and an ionic multicomponent complex, $[Cr^{I}(C_6H_6)_2^{\bullet+}] \cdot (C_{60}^{\bullet-}) \cdot 0.5[Pd(dbdtc)_2]$ (**5**) (Figure 1). The crystal structure of **5** together with optical (IR and UV−visible−NIR spectra) and magnetic properties of **1**−**5** (EPR and SQUID) are discussed. It was shown that unusual dimerization of $C_{60}^{\bullet-}$ is realized in **5** at the temperature lowest among those known for ionic complexes of C_{60}. The peculiarities of this low-temperature dimerization such as a hysteresis and a shift of dimerization temperature depending on cooling rate were studied and compared with those for the $C_{60}^{\bullet-}$ dimerization in other ionic complexes.

Experimental Section

Materials. Sodium dibenzyldithiocarbamate ($Na(dbdtc) \cdot xH_2O$) was purchased from Aldrich, bis(benzene)chromium $Cr(C_6H_6)_2$ from Strem Chemicals, and C_{60} of 99.98% purity from MTR Ltd. Sodium dibenzyldithiocarbamate was recrystallized from an acetonitrile/benzene mixture. $M(dbdtc)_2$ (M = Cu, Ni, Pd, Pt) was obtained by stirring 2 equiv of Na(dbdtc) and 1 equiv of anhydrous $CuBr_2$, $NiBr_2$, $PdCl_2$, and $PtCl_2$ salts (∼150 mg) (Aldrich) in 10 mL of acetonitrile on heating (50 °C) for 4 h. After cooling, $M(dbdtc)_2$ precipitated as brown (Cu), green (Ni), and light-yellow (Pd and Pt) powders together with NaBr or NaCl. The powders were dissolved in hot chlorobenzene, filtered off from NaBr or NaCl, and the solvent was removed to dryness in a rotary evaporator to afford pure $M(dbdtc)_2$ compounds with satisfactory elemental analyses (40−70% yield). Solvents were purified in argon atmosphere. *o*-Dichlorobenzene ($C_6H_4Cl_2$) and chlorobenzene (C_6H_5Cl) were distilled over CaH_2. Hexane and benzonitrile (C_6H_5CN) were distilled over Na/benzophenone. For the synthesis of air-sensitive **5**, solvents were degassed and stored in a glovebox. All manipulations with **5** were carried out in a MBraun 150B-G glovebox with controlled atmosphere and the content of H_2O and O_2 less than 1 ppm. The crystals were stored in a glovebox and were sealed in 2 mm quartz tubes for EPR and SQUID measurements under 10^{-5} Torr. KBr pellets for IR and UV−visible−NIR measurements of **5** were prepared in a glovebox.

Synthesis. The composition of **1**−**5** was determined from the elemental analysis (Table 1) and was justified for **5** by X-ray diffraction on a single crystal.

The crystals of **1** were obtained by the slow evaporation of chlorobenzene/benzonitrile (12:1) solution (13 mL) containing C_{60} (25 mg, 0.0347 mmol) and an equimolar amount of $Cu(dbdtc)_2$ (21 mg, 0.0347 mmol) during one week. The crystals precipitated were decanted from the benzonitrile solution (∼1 mL) and were washed with acetonitrile to afford black hexagonal plates with 70% yield.

Similar syntheses with $Ni(dbdtc)_2$, $Pd(dbdtc)_2$, and $Pt(dbdtc)_2$ did not afford crystals of the complexes with C_{60}, and only the crystals of the $C_{60}(C_6H_5Cl)_x$ solvate were found according to the IR spectrum. Because of this, we modified the synthetic procedure, adding an excess of ferrocene to the starting solution. The crystals

(5) (a) Crane, J. D.; Hitchcock, P. B.; Kroto, H. W.; Teylor, R.; Walton, D. R. M. *J. Chem. Soc. Chem. Commun*. **1992**, 1767. (b) Wan, W. C.; Liu, X.; Sweeney, G. M.; Broderick, W. E. *J. Am. Chem. Soc*. **1995**, *117*, 9580. (c) Konarev, D. V.; Khasanov, S. S.; Saito, G.; Vorontsov, I. I.; Otsuka, A.; Lyubovskaya, R. N.; Antipin, Yu. M. *Inorg. Chem*. **2003**, *42*, 3706. (d) Hönnerscheid, A.; Wüllen, L.; Jansen, M.; Rahmer, J.; Mehring, M. *J. Chem. Phys*. **2001**, *115*, 7161. (e) Konarev, D. V.; Khasanov, S. S.; Saito, G.; Otsuka A.; Yoshida Y.; Lyubovskaya R. N. *J. Am. Chem. Soc*. **2003**, *125*, 10074. (f) Hönnerscheid, A.; van Wüllen, L.; Dinnebier, R.; Jansen, M.; Rahmer, J.; Mehring, M. *Phys. Chem. Chem. Phys*. **2004**, *6*, 2454. (g) Ketkov, S. Yu.; Domrachev, G. A.; Ob'edkov, A. M.; Vasil'kov, A. Yu.; Yur'eva, L. P.; Mehner, C. P. *Russ. Chem. Bull*. **2004**, *53*, 1932.

(6) (a) Olmstead, M. M.; Costa, D. A.; Maitra, K.; Noll, B. C.; Phillips, S. L.; Van Calcar P. M.; Balch, A. L. *J. Am. Chem. Soc*. **1999**, *121*, 7090. (b) Boyd, P. D. W.; Hodgson, M. C.; Rickard, C. E. F.; Oliver, A. G.; Chaker, L.; Brothers, P. J.; Bolskar, R. D.; Tham F. S.; Reed, C. A. *J. Am. Chem. Soc*. **1999**, *121*, 10487. (c) Konarev, D. V.; Neretin, I. S.; Slovokhotov, Yu. L.; Yudanova, E. I.; Drichko, N. V.; Shul'ga, Yu. M.; Tarasov, B. P.; Gumanov, L. L.; Batsanov, A. S.; Howard J. A. K.; Lyubovskaya, R. N. *Chem. Eur. J*. **2001**, *7*, 2605. (d) Ishii, T.; Aizawa, N.; Kanehama, R.; Yamashita, M.; Sugiura, K.; Miyasaka, H. *Coord. Chem. Rev*. **2002**, *226*, 113.

(7) Hochmuth, D. H.; Michel, S. L. J.; White, A. J. P.; Williams, D. J.; Barrett A. G. M.; Hoffman, B. M. *Eur. J. Inorg. Chem*. **2000**, 593.

(8) (a) Konarev, D. V.; Zerza, G.; Scharber, M. C.; Sariciftci, N. S.; Lyubovskaya, R. N. *Mol. Crys. Liq. Crys*. **2005**, *427*, 3; 315. (b) Lopatin, D. V.; Rodaev, V. V.; Umrikhin, A. V.; Konarev, D. V.; Litvinov, A. L.; Lyubovskaya, R. N. *J. Mater. Chem*. **2005**, *15*, 657.

(9) Konarev, D. V.; Kovalevsky, A. Yu.; Lopatin, D. V.; Rodaev, V. V.; Umrikhin, A. V.; Yudanova, E. I.; Coppens, P.; Lyubovskaya, R. N.; Saito, G. *Dalton Trans*. **2005**, 1821.

(10) (a) Konarev, D. V.; Khasanov, S. S.; Otsuka, A.; Yoshida, Y.; Lyubovskaya, R. N.; Saito, G. *Chem. Eur. J*. **2003**, *9*, 3837. (b) Konarev, D. V.; Neretin, I. S.; Saito, G.; Slovokhotov, Yu. L.; Otsuka, A.; Lyubovskaya, R. N. *Dalton Trans.* **2003**, 3886. (c) Konarev, D. V.; Khasanov, S. S.; Vorontsov, I. I.; Saito, G.; Antipin, Yu. A.; Otsuka, A.; Lyubovskaya, R. N. *Chem. Commun*. **2002**, 2548. (d) Konarev, D. V.; Khasanov, S. S.; Saito, G.; Lyubovskaya, R. N. *Recent Res. Dev. Chem*. **2004**, *2*, 105. (e) Konarev, D. V.; Kovalevsky, A. Yu.; Khasanov, S. S.; Saito, G.; Otsuka, A.; Coppens, P.; Lyubovskaya, R. N. *Eur. J. Inorg. Chem*. **2005**, in press.

Table 1. Elemental Analysis Data for **1**−**5**

		elemental analysis, found/calcd			
N	complex	C, %	H, %	N, %	Cl, %
1	$Cu(dbdtc)_2 \cdot C_{60} \cdot 0.5(C_6H_5Cl)$	79.61	2.53	2.09	1.49
		80.58	2.24	2.02	1.28
2	$Ni(dbdtc)_2 \cdot C_{60} \cdot 0.5(C_6H_5Cl)$	81.94	2.57	2.06	1.11
		81.07	2.23	2.01	1.27
3	$Pd(dbdtc)_2 \cdot C_{60} \cdot 0.5(C_6H_5Cl)$	79.31	2.38	1.91	1.15
		78.21	2.17	1.96	1.24
4	$Pt(dbdtc)_2 \cdot C_{60} \cdot 0.5(C_6H_5Cl)$	75.32	2.36	1.87	1.17
		73.63	2.01	1.84	0.79
5	$[Cr(C_6H_6)_2] \cdot (C_{60}) \cdot 0.5[Pd(dbdtc)_2]$[a]	80.86[b]	2.37	1.22	−
		83.32	2.07	1.12	−

[a] The composition of the complex was consistent with the X-ray structure analysis on a single crystal. The unit cell parameters of several crystals from the synthesis were tested to justify the identity of the crystals in one synthesis. [b] The lack of carbon content can be a result of partial oxygenation of air-sensitive **5** while carrying out the elemental analysis.

of **2**−**4** were obtained by the slow evaporation of chlorobenzene/benzonitrile (12:1) solution (13 mL) containing C_{60} (25 mg, 0.0347 mmol), an equimolar amount of $M(dbdtc)_2$ (M = Ni, Pd, Pt) (20−25 mg, 0.0347 mmol), and Cp_2Fe (50 mg, 0.268 mmol) during one week. The crystals precipitated were decanted from the benzonitrile solution (∼1 mL) and were washed with acetonitrile to yield black hexagonal plates with 60−90% yield. According to the IR spectra, the crystals precipitated were found to be ferrocene-free and comprise only $M(dbdtc)_2$ (M = Ni, Pd, Pt), C_{60}, and solvent C_6H_5Cl molecules (Supporting Information).

The crystals of **5** were obtained by a slow diffusion of hexane (25 mL) in 18 mL of the $C_6H_4Cl_2$ solution containing C_{60} (25 mg, 0.035 mmol), $Pd(dbdtc)_2$ (40 mg, 0.054 mmol), and $Cr(C_6H_6)_2$ (12 mg, 0.057 mmol) in a glass tube 1.5 cm in diameter and 50 mL volume with a ground glass plug. The starting solution was prepared by dissolving all components by stirring at 60 °C for 4 h, and then the resulting solution was cooled to room temperature, filtered, and covered over with hexane. After 1 month, the crystals of **5** were formed on the wall of the tube. The solvent was decanted from the crystals precipitated, which were then washed with hexane to yield black needles with 60% yield.

General. UV−visible−NIR spectra were measured on a Shimadzu-3100 spectrometer in the 240−2600 nm range. FT-IR spectra were measured in KBr pellets with a Perkin-Elmer 1000 Series spectrometer (400−7800 cm^{-1}). A Quantum Design MPMS-XL SQUID magnetometer was used to measure static magnetic susceptibilities of **1** and **5** from 1.9 up to 300 K and for **5** from 300 down to 4 K at a 100 mT static magnetic field. A sample holder contribution (Θ) and core temperature independent diamagnetic susceptibility (χ_0) were subtracted from the experimental values. The values of Θ and χ_0 were calculated for **1** and **5** using the appropriate formula: $\chi_M = C/(T - \Theta) + \chi_0$. Two temperature ranges (before and after the transition) were used in the calculations for **5** (from 20 to 120 K and from 160 to 300 K). EPR spectra were recorded for **1** at room temperature (RT) and for **5** from RT down to 4 K and from 4 K up to RT with a JEOL JES-TE 200 X-band ESR spectrometer equipped with a JEOL ES-CT470 cryostat. Both slow cooling and heating were carried out within 4−6 h, whereas fast cooling was carried out only within 10 min from RT down to 100 K.

Crystal Structure Determination. Crystal data for **5**: $C_{174}H_{52}N_2S_4Cr_2Pd$, $M_r = 2508.82$, black needles, triclinic, space group $P\bar{1}$. The unit cell parameters are $a = 10.182(2)$ Å, $b = 15.225(3)$ Å, $c = 18.331(3)$ Å, $\alpha = 65.837(3)°$, $\beta = 74.733(3)°$, $\gamma = 76.867(3)°$, $V = 2478.1(8)$ Å^3, $Z = 1$, $D_c = 1.681$ g·cm^{-3}, $\mu = 0.554$ mm^{-1}, $F(000) = 1268.0$.

X-ray diffraction data for **5** were collected at 90(1) K using a Bruker SMART1000 CCD diffractometer installed at a rotating anode source (Mo Kα radiation, $\lambda = 0.71073$ Å) and equipped with an Oxford Cryosystems nitrogen gas-flow apparatus. The data were collected by the rotation method with 0.3° frame-width (ω scan) and 10 s exposure time per frame. Four sets of data (600 frames in each set) were collected, nominally covering half of the reciprocal space. The data were integrated, scaled, sorted, and averaged using the SMART software package.[22] In total, $N_{tot} = 17\,488$ reflections were measured up to $2\theta_{max} = 50.14°$; 8588 ($R_{int} = 0.050$) of them were independent. The structures were solved by the direct methods using SHELXTL NT Version 5.10.[23] The structure was refined by full-matrix least squares against F^2. Non-hydrogen atoms were refined in anisotropic approximation. Positions of hydrogen atoms were calculated geometrically. Subsequently, the positions of H-atoms were refined by the "riding" model with $U_{iso} = 1.2U_{eq}$ of the connected non-hydrogen atom. The least-squares refinement on F^2 was done to $R1[I > 2\sigma(I)] = 0.097$ for 6656 observed reflections with $F > 4\sigma(F)$, wR2 = 0.279 (826 parameters), final GOF = 1.110. The CCDC reference number is 275197.

Results and Discussion

1. Synthesis. Composition, elemental analysis of **1**−**4** are listed in Table 1. **1** was obtained by the evaporation of a chlorobenzene solution containing equimolar amounts of C_{60}

(11) Konarev, D. V.; Kovalevsky, A. Yu.; Li, X.; Neretin, I. S.; Litvinov, A. L.; Drichko, N. V.; Slovokhotov, Yu. L.; Coppens, P.; Lyubovskaya, R. N. *Inorg. Chem.* **2002**, *41*, 3638.
(12) Jian, F.; Wang, Z.; Bai, Z.; You, X.; Fun, H.-K.; Chinnakali K.; Razak, I. A. *Polyhedron* **1999**, *18*, 3401.
(13) Semkin, V. N.; Drichko, N. V.; Kimzerov, Yu. A.; Konarev, D. V.; Lyubovskaya, R. N.; Graja, A. *Chem. Phys. Lett.* **1998**, *295*, 266.
(14) Picher, T.; Winkler, R.; Kuzmany, H. *Phys. Rev. B* **1994**, *49*, 15879.
(15) Fritz, H. P.; Lüttke, W.; Stammreich, H.; Forneris, R. *Chem. Ber.* **1959**, *92*, 3246.
(16) Treichel, P. M.; Essenmacher, G. P.; Efner, H. F.; Klabunde, K. J. *Inorg. Chim. Acta* **1981**, *48*, 41.
(17) Dubois, D.; Kadish, K. M.; Flanagan, S.; Haufler, R. E.; Chibante, L. P. F.; Wilson, L. J. *J. Am. Chem. Soc.* **1991**, *113*, 4364.
(18) Dresselhaus, M. S.; Dresselhaus, G. In *Fullerene Polymers and Fullerene Polymer Composites*; Eklund, P. C., Rao, A. M., Eds.; Springer-Verlag; Berlin, 1999; pp 1−57.
(19) Rowland, R. S.; Taylor, R. *J. Phys. Chem.* **1996**, *100*, 7384.
(20) Elschenbroich, C.; Bilger, E.; Koch, J. *J. Am. Chem. Soc.* **1984**, *106*, 4297.
(21) (a) Lokaj, J.; Vrabel, V.; Kello. E. *Chem. Zvesti* **1984**, *38*, 313. (b) Riekkola, M.-L.; Pakkanen, T.; Niinisto, L. *Acta Chem. Scand. Ser. A.* **1983**, *37*, 807.
(22) SMART and SAINTPLUS, Area detector control and integration software, Version 6.01; Bruker Analytical X-ray Systems: Madison, WI, 1999.
(23) SHELXTL, An integrated system for solving, refining and displaying crystal structures from diffraction data, Version 5.10; Bruker Analytical X-ray Systems: Madison, WI, 1997.

Table 2. UV−Vis−NIR Spectra of the Starting Compounds and **1**−**5**

compounds	absorption bands, nm[a]		
	fullerene	$M(dbdtc)_2$	NIR range ($C_{60}^{\bullet-}$)
C_{60}	266s, 344, 470m, 605w		
$Cu(dbdtc)_2$		275s, 436s	
$Ni(dbdtc)_2$		326s, 635m	
$Cu(dbdtc)_2 \cdot C_{60} \cdot 0.5(C_6H_5Cl)$ (**1**)	262s, 337s, −	427m	
$Ni(dbdtc)_2 \cdot C_{60} \cdot 0.5(C_6H_5Cl)$ (**2**)	260s, 337s, 485w, 610w	∼670w	
$Pd(dbdtc)_2 \cdot C_{60} \cdot 0.5(C_6H_5Cl)$ (**3**)	261s, 340s, 480w, 610w		
$Pt(dbdtc)_2 \cdot C_{60} \cdot 0.5(C_6H_5Cl)$ (**4**)	261s, 340s, 480w, 610w		
$[Cr(C_6H_6)_2] \cdot (C_{60}) \cdot 0.5[Pd(dbdtc)_2]$ (**5**)	266s, 354s, −, 610w		933, 1073m

[a] s, strong; m, medium; w, weak.

and $Cu(dbdtc)_2$, whereas solvate with chlorobenzene ($C_{60} \cdot (C_6H_5Cl)_x$) was isolated in similar conditions with $Ni(dbdtc)_2$, $Pd(dbdtc)_2$, and $Pt(dbdtc)_2$ according to the IR spectra. The crystallization of **2**−**4** was provided by an addition of an excess of ferrocene, which however, was not inserted into the crystals precipitated. Previously, it was found that the excess of ferrocene provided the crystallization of solvent-free phases without ferrocene or new phases of fullerene complexes with ferrocene.[11] In the case of **2**−**4**, ferrocene probably promoted the decomposition of a fullerene solvate with chlorobenzene and, consequently, the formation of complexes with $M(dbdtc)_2$.

To prepare $[Cr(C_6H_6)_2^{\bullet+}] \cdot (C_{60}^{\bullet-}) \cdot 0.5[Pd(dbdtc)_2]$ (**5**) (Table 1), we used slow diffusion, in which $Cr(C_6H_6)_2$, C_{60} and the excess of $Pd(dbdtc)_2$ dissolved in $C_6H_4Cl_2$ were covered by hexane. In these conditions, **5** was formed instead of previously obtained $Cr(C_6H_6)_2 \cdot C_{60} \cdot 0.7(C_6H_4Cl_2)$.[5f] $Cu(dbdtc)_2$ was not used in the synthesis because of the reduction of Cu^{II} to Cu^{I} by $Cr(C_6H_6)_2$, which was accompanied by the color change from dark-brown to light-yellow characteristic of a Cu^{I} complex. Despite similar sizes and shapes, $M(dbdtc)_2$ and TBPDA form multicomponent complexes of different types. The $(D^+) \cdot (C_{60}^{\bullet-}) \cdot 2(TBPDA)$ complexes have large cavities to accommodate $Cp^*_2Cr^+$, $Cp^*_2Co^+$, or $TDAE^{\bullet+}$ cations, whereas smaller $Cr^{I}(C_6H_6)_2^{\bullet+}$ and Cp_2Co^+ (cobaltocenium) do not form such complexes.[10e] In contrast, $Pd(dbdtc)_2$ forms a complex with $C_{60}^{\bullet-}$ only together with $Cr^{I}(C_6H_6)_2^{\bullet+}$ countercations.

2. Neutral Complexes 1−4. The IR spectra of **1**−**4** are a superposition of those of C_{60}, $M(dbdtc)_2$, and C_6H_5Cl molecules (Supporting Information). IR-active bands of C_{60} at 527, 577, 1182, and 1429 cm^{-1} remain almost unchanged in the complexes (526, 577, 1182, and 1427−1428 cm^{-1}), showing no noticeable charge transfer to C_{60} in the ground state. The bands of $M(dbdtc)_2$ are shifted up to 10 cm^{-1} relative to starting donors, showing the changes in geometry of the $M(dbdtc)_2$ molecules in the complexes rather than charge transfer. The UV−visible−NIR spectra also justify a neutral ground state of the complexes (Table 2). The bands at 933 and 1073 nm characteristic of the C_{60} monoanion[3] are absent in the spectra of **1**−**4**. $Cu(dbdtc)_2$ has absorption with a maximum at 436 nm and the absorption tail up to 600 nm. This absorption is still observed in the spectrum of **1** at 427 nm (Table 2). A similar absorption spectrum was reported for $[Cu(dedtc)_2]_2 \cdot C_{60}$ with a maximum at 442 nm.[9] Photoexcitation of $Cu(dedtc)_2$ was shown to contribute to the generation of free charge carriers in $[Cu(dedtc)_2]_2 \cdot C_{60}$.[9] Therefore, the absorption of a donor component in the visible range is one of important factors, which define photoconductivity in solid fullerene complexes. Since $Ni(dbdtc)_2$ absorbs in the visible range with a maximum at 635 nm, the absorption of **2** at ∼670 nm was also attributed to $Ni(dbdtc)_2$. $Pd(dbdtc)_2$ and $Pt(dbdtc)_2$ do not have noticeable absorption in the visible range.

$Ni(dbdtc)_2$, $Pd(dbdtc)_2$, and $Pt(dbdtc)_2$ are EPR silent, and only $Cu^{II}(dbdtc)_2$ with a 1/2 ground state is paramagnetic and EPR active. Pristine $Cu(dbdtc)_2$ has an asymmetric EPR spectrum, which was simulated by two Lorentzian lines with $g_1 = 2.0515$ and $g_2 = 2.0295$ and line halfwidths (ΔH) of 8.52 and 5.76 mT. The EPR signal of **1** is also asymmetric and was simulated by two Lorentzian lines with $g_1 = 2.0521$ and $g_2 = 2.0362$ and ΔH of 4.32 and 2.18 mT (Supporting Information). The formation of a complex with C_{60} results in the narrowing of the EPR signal (by a factor of 2−2.5) with the retention of the *g*-factor values. This implies that the environment of Cu^{II} centers in $Cu(dbdtc)_2$ only weakly changes in **1** relative to the pristine donor. The changes in the EPR spectrum are more pronounced on the formation of $[Cu(dedtc)_2]_2 \cdot C_{60}$.[9] The EPR spectrum becomes a three-component instead of a two-component one of pristine donor. Such changes were attributed to the elongation of the axial Cu−S bond in the dimer due to the appearance of weak axial coordination of Cu^{II} to the C_{60} molecules.[9] Magnetic susceptibility of **1** follows the Curie−Weiss law, with a small Weiss constant of 0.15 K showing the absence of a magnetic interaction between Cu^{II} centers due to their large spatial separation. This agrees with the planar monomeric state of $Cu(dbdtc)_2$ in **1**. Dimeric Cu^{II} dialkyldithiocarbamates have a stronger antiferromagnetic interaction between Cu^{II} centers.[12]

3. Ionic Multicomponent Complex $[Cr^{I}(C_6H_6)_2^{\bullet+}] \cdot (C_{60}^{\bullet-}) \cdot 0.5[Pd(dbdtc)_2]$ (5). 3.1. IR- and UV−Visible−NIR Spectra. Three components were observed in the IR spectrum of **5** in KBr pellets. The absorption bands of C_{60} are positioned at 526, 575, 1182 cm^{-1}, and the split band has the maxima at 1387, 1392, and 1396 cm^{-1}. The $F_{1u}(4)$ mode of C_{60}, which is most sensitive to charge transfer to the C_{60} molecule is shifted from 1429 to 1387, 1392 and 1396 cm^{-1}, indicating charge transfer of ∼1 electron to the C_{60} molecule. The splitting of this mode can be due to the freezing of C_{60} molecular rotation even at RT and the decrease of its local symmetry. Similar splitting was observed due to the similar

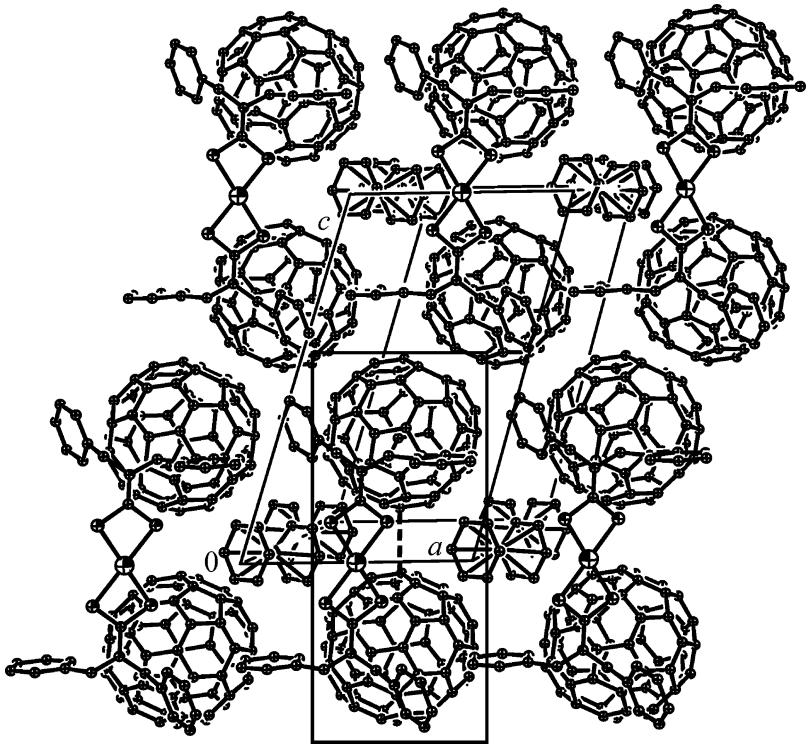

Figure 2. View of the crystal structure of **5** on the *ac* plane. One of the pairs from two $C_{60}^{\bullet-}$ radical anions is shown by the solid parallelogram. The shortest interfullerene C···C contact in the pair is depicted by a dashed line.

reason for some neutral complexes of C_{60}.[13] The integral intensity of the band at 575 cm^{-1} is essentially higher than that of the band at 526 cm^{-1}. This is also characteristic of $C_{60}^{\bullet-}$.[14] The bands at 419, 458, 787, 815, 971, 1011, 1140, and 1263 cm^{-1} were attributed to $Cr(C_6H_6)_2$. Two bands of $Cr(C_6H_6)_2$ are sensitive to charge transfer and are shifted from 459 and 490 cm^{-1} in the neutral state to 419 and 460 cm^{-1} in ionic $(Cr^{I}(C_6H_6)_2^{\bullet+})(I^-)$.[15] Similar shifts of the bands in the spectrum of **5** (419 and 458 cm^{-1}) also indicate the formation of $Cr^{I}(C_6H_6)_2^{\bullet+}$ radical cations, which is possible due to that the first redox potential of $Cr(C_6H_6)_2$ ($E^{+}/0 = -0.72$ V vs SCE[16]) is more negative than that of C_{60} ($E^{0/-} = -0.44$ V vs SCE[17]). The remaining absorption bands were attributed to $Pd(dbdtc)_2$ (Supporting Information). The UV−visible−NIR spectrum of **5** (Table 2) justifies the formation of $C_{60}^{\bullet-}$ from characteristic bands at 933 and 1073 nm. The additional bands in IR and UV−visible−NIR ranges, which must accompany the dimerization or polymerization of $C_{60}^{\bullet-}$[18] are absent, indicating their monomeric state at RT.

3.2. Crystal Structure. The crystal structure of **5** was determined at 90 K. It should be noted that a single crystal to be measured was cooled very fast from RT down to 90 K (within 10 s). The complex has a triclinic lattice. $C_{60}^{\bullet-}$, $Cr^{I}(C_6H_6)_2^{\bullet+}$, and $Pd(dbdtc)_2$ are completely ordered at 90 K; $C_{60}^{\bullet-}$ and $Cr^{I}(C_6H_6)_2^{\bullet+}$ radical ions occupy general positions, while $Pd(dbdtc)_2$ is located in a special position with the Pd atom being on a center of symmetry.

The complex has layered packing, in which strongly puckered layers of $C_{60}^{\bullet-}$ alternate with the layers composed of neutral $Pd(dbdtc)_2$ molecules along the *b* direction (Figure 2). $Cr^{I}(C_6H_6)_2^{\bullet+}$ radical cations are arranged between $C_{60}^{\bullet-}$ and $Pd(dbdtc)_2$ layers in the voids formed by two $Pd(dbdtc)_2$ molecules and four $C_{60}^{\bullet-}$ radical anions (Figure 2).

Within a fullerene layer, the pairs of $C_{60}^{\bullet-}$ can be outlined (solid parallelogram in Figure 2) with a center−to−center interfullerene distance of 10.16 Å. There is one shortened van der Waals interfullerene C···C contact of 3.092(2) Å in the pairs (dashed line in Figure 2). This contact is essentially longer than the intercage C−C bond in the $(C_{60}^-)_2$ dimer (1.597 Å[5e]). However, it is noticeably shorter than the sum of van der Waals radii of two carbon atoms (3.42 Å[19]). In addition to adjacent fullerenes in the pair, each $C_{60}^{\bullet-}$ has another four neighboring $C_{60}^{\bullet-}$ radical anions within the layer. Two neighbors are positioned on the same level along the *a* direction (Figure 2) with a center-to-center distance of 10.18 Å, and the shortest interfullerene C···C contacts are in the 3.69−3.76 Å range (longer than 3.42 Å). Two other neighbors are positioned approximately along the *c* axis with a center-to-center distance of 9.92 Å. However, the shortest C···C contacts (3.39−3.75 Å) are noticeabely longer than the interfullerene C···C distance in the pairs (Figure 2).

Each fullerene pair is surrounded by four $Cr^{I}(C_6H_6)_2^{\bullet+}$ radical cations, which form shortened van der Waals C···C and H···C contacts in the 3.23−3.56 and 2.65−2.92 Å ranges (Figures 2 and 3). The $C_{60}^{\bullet-}$ radical anions from one pair form van der Waals C···C contacts (3.30−3.50 Å) with benzyl groups of two $Pd(dbdtc)_2$ molecules lying above and below a fullerene layer (dashed lines in Figure 3). The central PdS_4 fragment does not form any shortened contacts with $C_{60}^{\bullet-}$ and $Cr^{I}(C_6H_6)_2^{\bullet+}$ radical ions; therefore, $Pd^{II}(dbdtc)_2$ does not coordinate to $C_{60}^{\bullet-}$ in contrast to $Co^{II}TPP$, which forms diamagnetic σ-bonded ($Co^{II}TPP$·fullerene$^-$) anions.[10a]

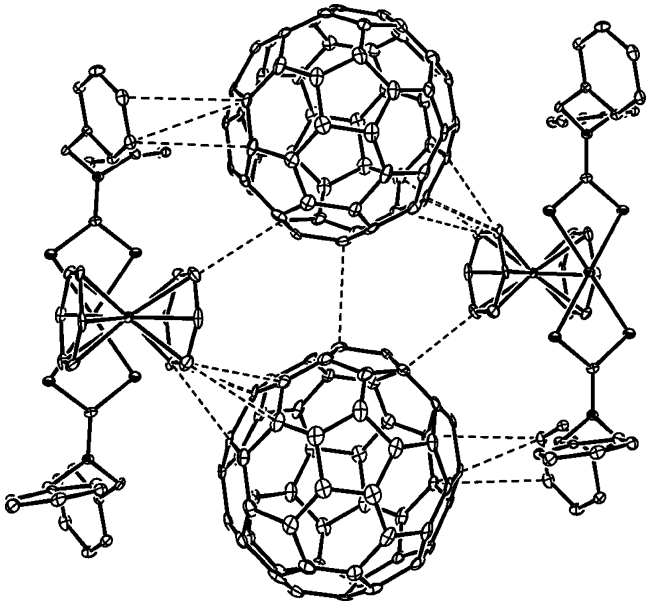

Figure 3. Van der Waals contacts in the crystal structure of **5** between $Pd(dbdtc)_2$, $C_{60}^{\bullet-}$, and $Cr(C_6H_6)_2^{\bullet+}$ radical ions (dashed lines).

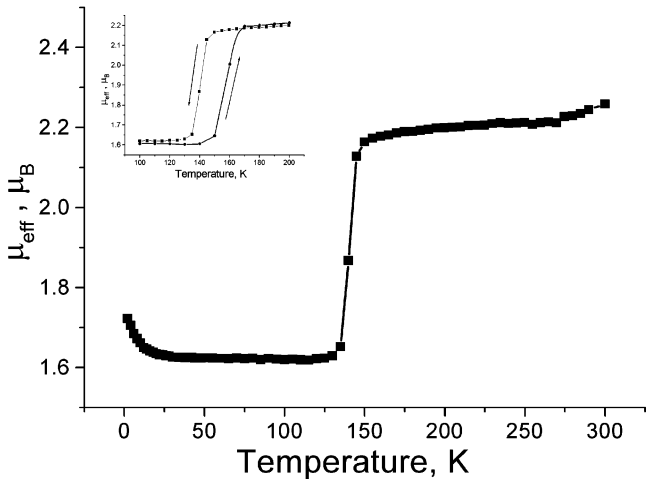

Figure 4. Effective magnetic moment on slow cooling **5** in the 300−1.9 K range. The insert shows the magnetic hysteresis in the 100−200 K range.

The central $(NCS_2)_2Pd$ fragment of the $Pd(dbdtc)_2$ molecule is planar (the dihedral angle between two NCS_2Pd planes is 180°). The averaged lengths of the S−Pd bonds are 2.325 Å.

3.3. Magnetic Properties of 5. The complex manifests a symmetric Lorentzian EPR signal at RT with $g = 1.9934$ and a line halfwidth (ΔH) of 4.06 mT. This signal has a g-factor intermediate between those characteristic of monomeric $C_{60}^{\bullet-}$ ($g = 1.9996-2.0000$)[1b,1c] and $Cr^{I}(C_6H_6)_2^{\bullet+}$ ($g = 1.9860$)[20] and was attributed to a resonating signal between these radical ions due to direct exchange coupling. Similar resonating EPR signals were observed in monomeric high-temperature phases of $Cr(C_6H_6)_2 \cdot C_{60} \cdot 0.7(C_6H_4Cl_2)$ and $Cr(C_6H_6)_2 \cdot C_{60} \cdot C_6H_5CN$,[5e] as well as in ionic complexes of C_{60} with other substituted bis(arene)chromium compounds.[5d,5g] The RT magnetic moment of **5** is 2.26 μ_B (Figure 4). This value is close to 2.45 μ_B (the value estimated for the system of two 1/2 spins per formula unit), implying the contribution from both $C_{60}^{\bullet-}$ and $Cr^{I}(C_6H_6)_2^{\bullet+}$ radical ions.

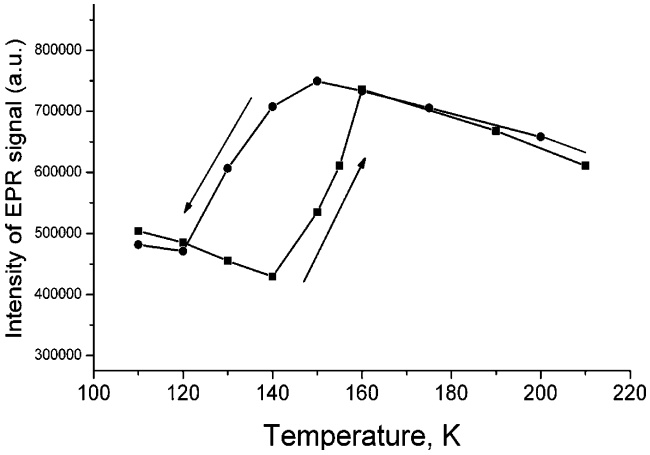

Figure 5. The changes in the integral intensity of the EPR signal of **5** on slow cooling and heating.

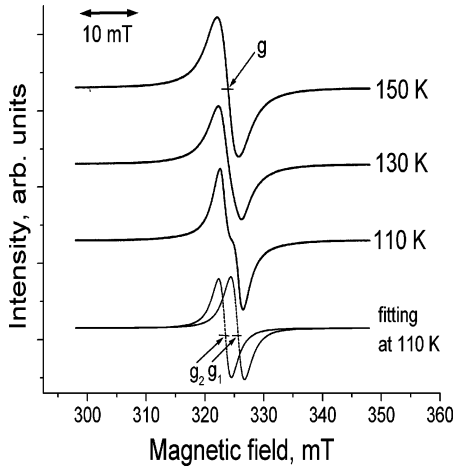

Figure 6. The splitting of the EPR signal from **5** upon the dimerization of $C_{60}^{\bullet-}$ in the 150−110 K range on slow cooling.

3.4. Peculiarities of the Formation of $(C_{60}^{-})_2$ Dimers in 5. The magnetic moment of **5** is only weakly temperature dependent on slow cooling (within 4−6 h) from RT down to 150 K and below 150 K decreases down to 1.62 μ_B (130 K) (Figure 4). This value is close to the contribution of one 1/2 spin per formula unit (1.73 μ_B). Above and below the transition, magnetic susceptibility of **5** follows the Curie−Weiss law with small Weiss constants (−0.3 and 0.2 K, respectively). EPR measurements are in agreement with SQUID data. The EPR signal remains unchanged down to 150 K ($g = 1.9929$ and $\Delta H = 3.61$ mT). The integral intensity of the EPR signal abruptly decreases by a factor of 2 at 150−120 K (Figure 5) and the signal splits into two lines with $g_1 = 1.9960$ ($\Delta H = 2.24$ mT) and $g_2 = 1.9826$ ($\Delta H = 2.32$ mT) at 120 K (Figure 6). Two lines have nearly temperature independent g-factors and line halfwidths down to 4 K ($g_1 = 1.9967$ and $g_2 = 1.9839$ with $\Delta H = 2.33$ and 2.34 mT), justifying the attribution of this signal to $Cr^{I}(C_6H_6)_2^{\bullet+}$.[20] A similar signal was observed in a dimeric phase of $Cr(C_6H_6)_2 \cdot C_{60} \cdot C_6H_5CN$ below 160 K ($g_1 = 1.9949$ and $g_2 = 1.9835$ at 4 K), whereas the signal in a dimeric phase of $Cr(C_6H_6)_2 \cdot C_{60} \cdot 0.7(C_6H_4Cl_2)$ is a single Lorentzian line down to 4 K.[5e] Thus, below 120 K, spins in **5** are localized on $Cr^{I}(C_6H_6)_2^{\bullet+}$ and the transition is associated with

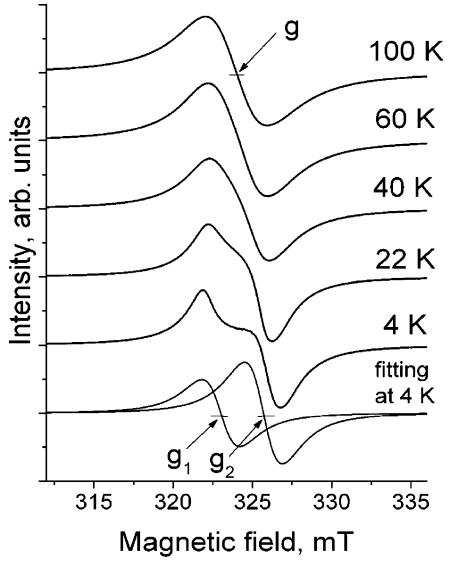

Figure 7. The EPR spectrum of **5** (100−4 K) upon fast cooling from RT down to 100 K.

the reversible formation of diamagnetic and EPR-silent single-bonded $(C_{60}^{-})_2$ dimers. Spin and magnetic susceptibility measurements on slow heating indicate the transition to be reversible with the shift to higher temperatures (150−170 K). Therefore, the hysteresis is 20 K (Figure 4, insert, and Figure 5). The crystals of **5** were also fast cooled from RT down to 100 K (within 10 min). In this case, the EPR signal indicates the retention of the monomeric phase even at 100 K ($g = 1.9930$ and $\Delta H = 3.87$ mT) (Figure 7). The signal remains unchanged down to 60 K (Figure 7) and only below 60 K splits into two components ($g_1 = 1.9991$ and $\Delta H = 2.38$ mT and $g_2 = 1.9826$ and $\Delta H = 2.39$ mT at 4 K), suggesting the dimerization of $C_{60}^{\bullet-}$. Similar splitting is observed upon the dimerization of $C_{60}^{\bullet-}$ on slow cooling of **5** in the range 150−120 K (Figure 6). Thus, fast cooling essentially lowers dimerization temperature.

Conclusion

In contrast to the C_{60} complex with butterfly-shaped $[Cu(dedtc)_2]_2$ dimers,[9] different $M(dbdtc)_2$ ($M = Cu^{II}$, Ni^{II}, Pd^{II}, and Pt^{II}) most probably form complexes with C_{60} (**1**−**4**) in planar conformation of the central $(NCS_2)_2M$ fragment adopting to spherical C_{60} molecules by flexible benzyl substituents. Planar conformation is known to be peculiar for $Ni(dbdtc)_2$, $Pd(dbdtc)_2$, and $Pt(dbdtc)_2$[21] and can also be realized for $Cu(dbdtc)_2$ due to the repulsion of bulky benzyl substituents. Two of the four dibenzyldithiocarbamates have absorption in the visible range, their complexes with C_{60} can be photoactive similarly to $[Cu(dedtc)_2]_2 \cdot C_{60}$,[9] and now this work is in progress. Ionic $[Cr^{I}(C_6H_6)_2^{\bullet+}] \cdot (C_{60}^{\bullet-}) \cdot 0.5[Pd(dbdtc)_2]$ (**5**) contains neutral $Pd(dbdtc)_2$, $C_{60}^{\bullet-}$ radical anions, and $Cr^{I}(C_6H_6)_2^{\bullet+}$ radical cations. The crystal structure of **5** (90 K) reveals layered packing with the alternation of strongly puckered $C_{60}^{\bullet-}$ layers with those of $Pd(dbdtc)_2$. $Cr^{I}(C_6H_6)_2^{\bullet+}$ radical cations are arranged between the layers (Figure 2). The radical anions form pairs within the $C_{60}^{\bullet-}$ layers with the shortest interfullerene C···C contact of 3.092(2) Å (Figure 2). Thus, $C_{60}^{\bullet-}$ radical anions are monomeric at 90 K. However, they can dimerize in the direction of this contact within the pairs. SQUID and EPR measurements indicate the formation of $(C_{60}^{-})_2$ dimers below 150−130 K on slow cooling and their dissociation above 150−170 K on heating (Figures 4 and 5). A symmetric EPR signal with $g = 1.9934$ attributable to a resonating signal between $C_{60}^{\bullet-}$ and $Cr^{I}(C_6H_6)_2^{\bullet+}$ radical ions changes to an asymmetric EPR signal with two lines with $g_1 = 1.9959$ and $g_2 = 1.9830$ characteristic of isolated $Cr^{I}(C_6H_6)_2^{\bullet+}$ (Figure 6). The dissociation temperature for the $(C_{60}^{-})_2$ dimers in **5** and their stability are low in comparison with those for other ionic complexes of C_{60} (160−250 K).[5d−g] Two peculiarities were found for such low-temperature dimerization. The dimerization in **5** has a larger hysteresis of 20 K, whereas in $Cp^*_2Cr \cdot C_{60} \cdot (C_6H_4Cl_2)_2$ with the dimerization temperature above 200 K, the hysteresis was smaller than 2 K.[5e] Fast cooling from RT down to 100 K completely suppresses dimerization, and according to EPR, it is observed only below 60 K (Figure 7). The crystal for a X-ray diffraction experiment was fast cooled from RT down to 90 K, and this can be a reason for the retention of a monomeric phase of **5** at 90 K.

Acknowledgment. The work was partly supported by a Grant-in-Aid Scientific Research from the Ministry of Education, Culture, Sports, Science and Technology, Japan (152005019, 21st Century COE, and Elements Science 12CE2005) and the RFBR Grant No. 03-03-32699a.

Supporting Information Available: Crystallographic data in CIF format for **5**, data of IR spectra for starting compounds and **1**−**5** (Table 1), UV−visible−NIR spectra for complexes **1**−**3** and **5**, and EPR spectra for **1** and $Cu(dbdtc)_2$ (Figures 1−5). This material is available free of charge via the Internet at http://pubs.acs.org.

IC051261I